Numerical Simulation of a Efficient Solar-Powered Ventilation System

Faouzi Nasri

Mechanical Engineering Department, College of Engineering, University of Bisha, Bisha, Saudi Arabia
fnasri@ub.edu.sa (corresponding author)

ABSTRACT

The objective of this study is to conduct a numerical analysis of a small-scale solar ventilation-air conditioning system operating under the meteorological conditions of Bisha, Saudi Arabia. The primary objective of the proposed system is to provide sustainable and comfortable thermal conditions. To achieve this objective, the system recovers the heat wasted by the solar ventilation process and reuses it to power the desiccant dehumidification process. The solar chimney features a lateral (vertical) wall design, and a comparative performance investigation of two solar chimney designs (conventional vs original) is conducted. Mathematical models of the ventilated room and solar chimney are developed, and numerical simulations are carried out to evaluate the performance of each solar chimney design. The study aims to assess the ability of each design to maintain indoor thermal comfort through the analysis of air distribution temperature and air streamlines. The results of the performance comparison revealed that the proposed solar chimney design outperformed the conventional design in terms of thermal and ventilation performance. The proposed solar chimney design, with its lateral (vertical) wall, was also found to be more effective in maintaining indoor thermal comfort than the conventional design. The simulations showed that the proposed design produced a more uniform air distribution temperature within the ventilated room, resulting in improved comfort levels. Additionally, the proposed design was found to have a more efficient airflow pattern, with fewer areas of stagnant airflow. These results suggest that the proposed solar ventilation-air conditioning system has the potential to provide sustainable and comfortable thermal conditions in small-scale buildings.

Keywords-solar chimney; ventilation; mathematical modeling; numerical simulation

I.   INTRODUCTION

Changes in operating conditions, such as flow rate, porosity, and inlet air temperature, have a significant impact on the amount of mass and heat transfer that occurs during sorption phenomena between the air and adsorbent medium. To design an efficient dehumidification system, it is essential to accurately determine the influence of the initial moisture content of the adsorbent. Recent literature has explored this topic and offers several interesting works that examine the influence of operating conditions on mass and heat transfer.

Authors in [1] investigated the impact of rotational speed on the performance of the desiccant wheel, which was characterized by the dehumidification effectiveness, dehumidification coefficient of performance, and sensible energy ratio. They also examined the influence of process air temperature and humidity inlets, regeneration air temperature, and the mass flow rate ratio of regeneration and process air on the optimal rotational velocity of the desiccant wheel. The authors discovered that the optimal rotational velocity for maximizing the dehumidification performance of the desiccant wheel ranged from 5 to 10 revolutions per hour, depending on the specific operating conditions. Additionally, they observed

that the sensible energy ratio increased monotonically with an increase in the rotational velocity.

Authors in [2] attempted to determine the optimal angle for achieving maximum airflow through natural ventilation in a solar chimney. They developed a model that allowed for the consideration of various parameters such as air velocity and temperature variation within the chimney. Authors in [3] used numerical analysis to investigate the temperature of the internal air in a solar greenhouse. They found that the temperature varied depending on several factors, including climate conditions, location, number of covers, and the shape of the greenhouse. It was also suggested that roofs could be utilized to generate electricity. Authors in [4] devised and analyzed a solar chimney system in a residential building that included a humidification and dehumidification desalination unit. The design aimed to facilitate ventilation and fresh water production through desalination. Authors in [5] proposed a solar energy-powered air conditioning system that utilized a façade acting as a solar chimney. The system used the heat from the solar chimney to facilitate the dehumidification process and drive an adsorption chiller. Authors in [6] conducted a numerical investigation on the effect of the inclination angle of the solar chimney and simulated the variation of the ventilation rate for different angles. They found

that an inclination angle of 45° to 70° was optimal for a latitude of 28.4°. Authors in [7] examined the impact of meteorological conditions on the daily incident solar flux on the facades of a building in the Adrar region of South Algeria. Authors in [8] carried out a theoretical study of a vertical facade solar chimney. Authors in [9-10] developed correlations to estimate a new pair of independent effectiveness parameters for desiccant wheels and investigated the influence of atmospheric pressure on heat and mass transfer within the wheels. Authors in [11] proposed a solar hybrid system for water desalination, air conditioning, and electricity production. Authors in [12] conducted a numerical and experimental study of a solar chimney and found that ambient air velocities greater than 2 m/s improved the air velocity in the ducts. Authors in [13] performed experiments on solar chimney thermal performance for natural ventilation and observed the impact of the pressure difference between input and output on the air velocity. Authors in [14] investigated the thermal comfort in a building obtained through a solar chimney in cold weather and found that indoor thermal comfort was maintained even with low solar intensity and ambient temperature. Authors in [15] compared different configurations of solar chimneys to determine the most efficient one. Authors in [16] investigated the solar energy potential and carried out an economic study of a 5 kW rooftop photovoltaic system in Botswana. Many researchers have proposed hybrid systems for air conditioning, electricity production, and desalination.

In this work, a proposed design of the studied system will be developed. The governing equations are presented and the results are discussed.

II. PROBLEM STATMENT

In Figure 1, the design proposal involves linking solar ventilation and solar desiccant air-conditioning. The coupling of these two systems is achieved by harnessing the waste heat generated by the solar ventilation system and using it to drive the desiccant dehumidification process. The conditioned room is naturally ventilated by a wall-mounted solar chimney that is oriented towards the south, and is also conditioned through a solar desiccant air-conditioning system.
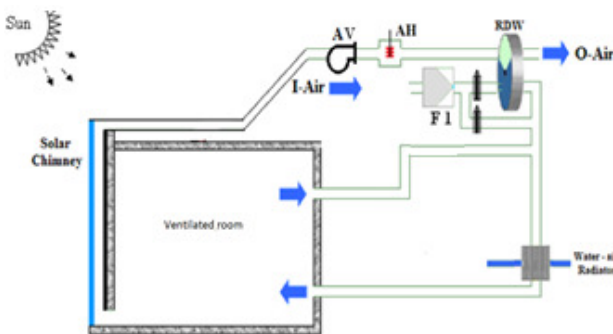

Fig. 1.   The proposed approach for a solar-powered ventilation-air conditioning system design.

To maintain a room temperature of 25°C, the proposed system utilizes a wall-mounted solar chimney that uses the greenhouse effect to heat up the air gap and create a pressure difference. This drives the hot air from the conditioned room

outlet towards the regeneration part of the Rotary Desiccant Wheel (RDW), allowing for desorption of the adsorbent in the RDW. In situations where the regeneration air is not hot enough, such as during night time, cloudy days, early morning, or late evening, an Auxiliary Heater (AH) and blower (AV) may be used to heat and drive the air from the chimney outlet. The system also incorporates a renewal inlet air (I-Air) that is first drawn from outside, filtered through F1, and then dehumidified using the desiccant in the adsorption part of the RDW. If the renewal inlet air (I-Air) has low relative humidity and is already dry, there is no requirement for dehumidification, and the Rotary Desiccant Wheel (RDW) can be bypassed. The renewal dehumidified air and room air are then mixed to obtain the process air, which is cooled through the water-air radiator (heat exchanger). The cooled process air is then filtered through F2 and injected into the conditioned room. Solar energy is harnessed using photovoltaic panels oriented towards the south to generate electricity to power all the electrical components of the proposed design, including blowers, auxiliary blower, desiccant wheel mechanical rotation, and possibly an auxiliary heater. The room to be ventilated has two openings, one providing direct access to fresh air intake, and the other used to release stale air to the solar chimney. The continuity equation, the momentum equations along the x and y axis and the energy conservation equation are stated as follows:

Continuity equation:

$$\frac{\partial(u)}{\partial x} + \frac{\partial(v)}{\partial y} = 0 \tag{1}$$

x- and y-Momentum:

$$\frac{\partial(uu)}{\partial x} + \frac{\partial(vu)}{\partial y} = -\frac{1}{\rho}\frac{\partial P}{\partial x} + \frac{1}{\rho}\frac{\partial}{\partial x}\left(\left(\mu + \mu_t\right)\frac{\partial u}{\partial x}\right) + \frac{1}{\rho}\frac{\partial}{\partial y}\left(\left(\mu + \mu_t\right)\frac{\partial u}{\partial y}\right) - \frac{2}{3}\frac{\partial k}{\partial x} \tag{2}$$

$$\frac{\partial(uv)}{\partial x} + \frac{\partial(vv)}{\partial y} = -\frac{1}{\rho}\frac{\partial P}{\partial y} + \frac{1}{\rho}\frac{\partial}{\partial x}\left(\left(\mu + \mu_t\right)\frac{\partial v}{\partial x}\right) + \frac{1}{\rho}\frac{\partial}{\partial y}\left(\left(\mu + \mu_t\right)\frac{\partial v}{\partial y}\right) - \frac{2}{3}\frac{\partial k}{\partial y} + g\beta\left(T - T_0\right) \tag{3}$$

Energy conservation equation:

$$\frac{\partial(uT)}{\partial x} + \frac{\partial(vT)}{\partial y} = \frac{1}{\rho}\frac{\partial}{\partial x}\left(\left(\frac{\mu}{\Pr} + \frac{\mu_t}{\Pr_t}\right)\frac{\partial T}{\partial x}\right) + \frac{1}{\rho}\frac{\partial}{\partial y}\left(\left(\frac{\mu}{\Pr} + \frac{\mu_t}{\Pr_t}\right)\frac{\partial T}{\partial y}\right) \tag{4}$$

The equations governing the transport of turbulent kinetic energy (k) and turbulent energy dissipation (ε) are fundamental equations used in turbulent fluid mechanics. The equations are typically expressed below.

Turbulent kinetic energy:

$$\frac{\partial(uk)}{\partial x} + \frac{\partial(vk)}{\partial y} = \frac{1}{\rho}\frac{\partial}{\partial x}\left(\left(\mu + \frac{\mu_t}{\Pr_k}\right)\frac{\partial k}{\partial x}\right) + \frac{1}{\rho}\frac{\partial}{\partial y}\left(\left(\mu + \frac{\mu_t}{\Pr_k}\right)\frac{\partial k}{\partial y}\right) + \frac{1}{\rho}\left(G_k + G_b\right) - \varepsilon \tag{5}$$

Turbulence dissipation:

$$\frac{\partial(u\varepsilon)}{\partial x}+\frac{\partial(v\varepsilon)}{\partial y}=\frac{1}{\rho}\frac{\partial}{\partial x}\left(\left(\mu+\frac{\mu_t}{\Pr_\varepsilon}\right)\frac{\partial\varepsilon}{\partial x}\right)+\frac{1}{\rho}\frac{\partial}{\partial y}\left(\left(\mu+\frac{\mu_t}{\Pr_\varepsilon}\right)\frac{\partial\varepsilon}{\partial y}\right)$$
$$+C_{1\varepsilon}\frac{\varepsilon}{\rho k}\left(G_k+C_{3\varepsilon}G_b\right)-C_{2\varepsilon}\frac{\varepsilon^2}{k} \qquad (6)$$

with $C_{1\varepsilon}$, $C_{2\varepsilon}$ and $C_{3\varepsilon}$ values of 1.44, 1.92, and 0.09, respectively, and are empirical constants [17], $\Pr_k$ and $\Pr_\varepsilon$ are the turbulent Prandtl numbers for the variables k and ε having values of 1.0 and 1.3, respectively [13], and G_k indicates the gradients in mean velocity, are the turbulent Prandtl numbers for the variables:

$$G_k=\mu_t\left(\frac{\partial u_i}{\partial x_j}+\frac{\partial u_j}{\partial x_i}\right)\frac{\partial u_i}{\partial x_j}-\frac{2}{3}\rho k\delta_{ij}\frac{\partial u_i}{\partial x_j} \qquad (7)$$

where G_b represents the production of the turbulent kinetic energy due to the buoyancy:

$$G_b=\beta g_i\frac{\mu_t}{\Pr_t}\frac{\partial T}{\partial x_i} \qquad (8)$$

Equations (1)-(8) are numerically implemented to assess the air temperature distribution and the air streamlines in the conditioned room.

The proposed solar chimney consists of two key components: a tunnel and a collector (absorber and glass cover). When creating an energy model for the solar chimney, several necessary hypotheses are taken into account, including:

- The absorber is uniformly heated: It is assumed that the absorber is heated uniformly by the sun's radiation, which allows for simplified calculations.

- The solar collector is facing south: The solar collector is assumed to be oriented towards the south, and the influence of the sun's azimuth angle fluctuation is neglected. This simplifies the calculations but may not accurately represent the actual solar radiation that the collector receives.

- The impact of the turbine on the airflow turbulence is disregarded: It is assumed that the airflow through the solar chimney is steady, and the impact of the turbine on airflow turbulence is ignored. This simplifies the analysis but may not represent the actual airflow behavior.

- Airflow resistance losses are ignored: The losses due to air flow resistance are disregarded, which may not represent the actual pressure drop through the solar chimney.

Energy balance equation for the glass cover:

$$\alpha_{gls}I=h_{rd,gls-sky}\left(T_{gls}-T_{sky}\right)+h_{cv,gls-top}\left(T_{gls}-T_{amb}\right)$$
$$+h_{cv,gls-f}\left(T_{gls}-T_f\right)+h_{rd,gls-abs}\left(T_{gls}-T_{abs}\right) \qquad (9)$$

Energy balance equation for the absorber:

$$\tau_{gls}\alpha_{gls}I=U_{abs-b}\left(T_{abs}-T_b\right)$$
$$+h_{cv,abs-f}\left(T_{abs}-T_f\right)+h_{rd,abs-gls}\left(T_{abs}-T_{gls}\right) \qquad (10)$$

Energy balance equation for the air flow in the collector:

$$\frac{\dot{m}_f C_{p,f}}{\xi S}\left(T_f-T_r\right)=$$
$$\left[-h_{cv,gls-f}\left(T_f-T_{gls}\right)-h_{cv,abs-f}\left(T_f-T_{abs}\right)\right] \qquad (11)$$

Axial mean air temperature equation:

$$T_f=\xi T_{f,\text{out}}+(1-\xi)T_{f,\text{in}} \qquad (12)$$

where ξ is a constant that is suggested to be 0.74 [19].

The heat transfer coefficients involved in (9)-(11) can be found in [18]. The air temperature at the entrance of the regeneration portion of the rotating desiccant wheel is obtained numerically using (9)–(12).

III. NUMERICAL RESULTS AND DISCUSSION

Figure 2 depicts the evolution of realistic solar irradiance on June 1 and July 15, 2022, from 07:00 to 18:00. Parabolic trends of solar irradiance are imposed by the sun path. On June 1st, 2022, the solar irradiance starts with 240 W/m² at 07:00 to reach 800 W/m² at 13:00 and finally falls to 470 W/m² at 18:00. On July 15th, 2022, the solar irradiance starts with 330 W/m² at 07:00 to reach 910 W/m² at 12:00-13:00 and finally falls to 480 W/m² at 18:00. Based on Figure 3, the evolution of the realistic ambient temperature on June 1 and July 15, 2022, from 07:00 to 18:00, can be described as follows: On June 1st, 2022: The ambient temperature starts at 27°C at 07:00 and rises rapidly to 39°C at 13:00. After 13:00, the temperature begins to decrease slowly and falls to 32°C at 18:00. On July 15th, 2022: The ambient temperature starts at 29°C at 07:00 and increases rapidly to 42°C at 14:30. After 14:30, the temperature begins to drop slowly and falls to 39°C by 18:00.
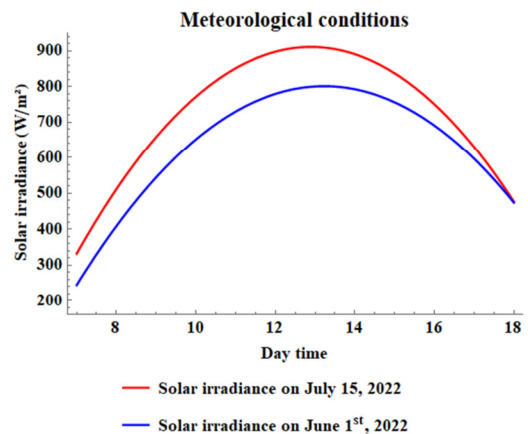

Fig. 2.   Solar irradiance on June 1 and July 15, 2022.

Figures 4-6 provide important information regarding the thermal performance of the solar chimney. Specifically, these figures depict the inlet chimney air temperature, as well as the minimum and maximum required regeneration air temperature. This information allows for an assessment of the appropriateness of the outlet chimney air temperature in relation to the thermal performance of the solar chimney.
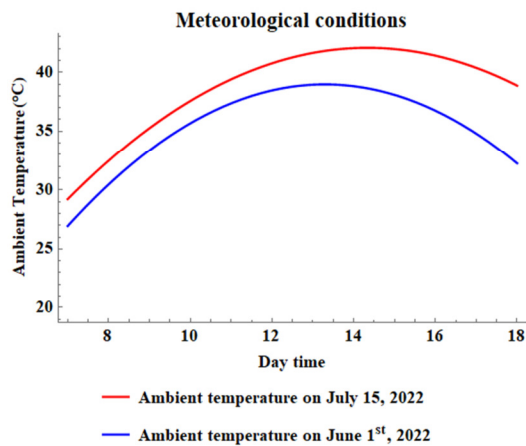
Fig. 3.   Simulation study of the realistic ambient temperatures on June 1 and July 15, 2022.

Figure 4 provides important information regarding the evolution of the outlet chimney air temperature on June 1st and July 15th, 2022, from 07:00 to 18:00. The Figure indicates that the glass transmittance, chimney air gap, and chimney area were set to 0.799, 5 mm, and 3×3 m² respectively. According to the Figure, the outlet chimney air temperature becomes appropriate as regeneration air from 08:30 on June 1, 2022, and from 09:30 to 17:00 on July 15, 2022. This suggests that the solar ventilation system is effective in providing the required ventilation and cooling during these periods, as well as providing hot air for the dehumidification stage of the active desiccant air conditioning system. It is important to note that the periods lasting from 08:30-09:30 to 18:00 are the most critical periods when the solar ventilation as passive air-conditioning and active desiccant air conditioning system are required to maintain the desired room temperature. During these periods, the outlet chimney air temperature is appropriate, which indicates that the solar ventilation system is operating efficiently and effectively.
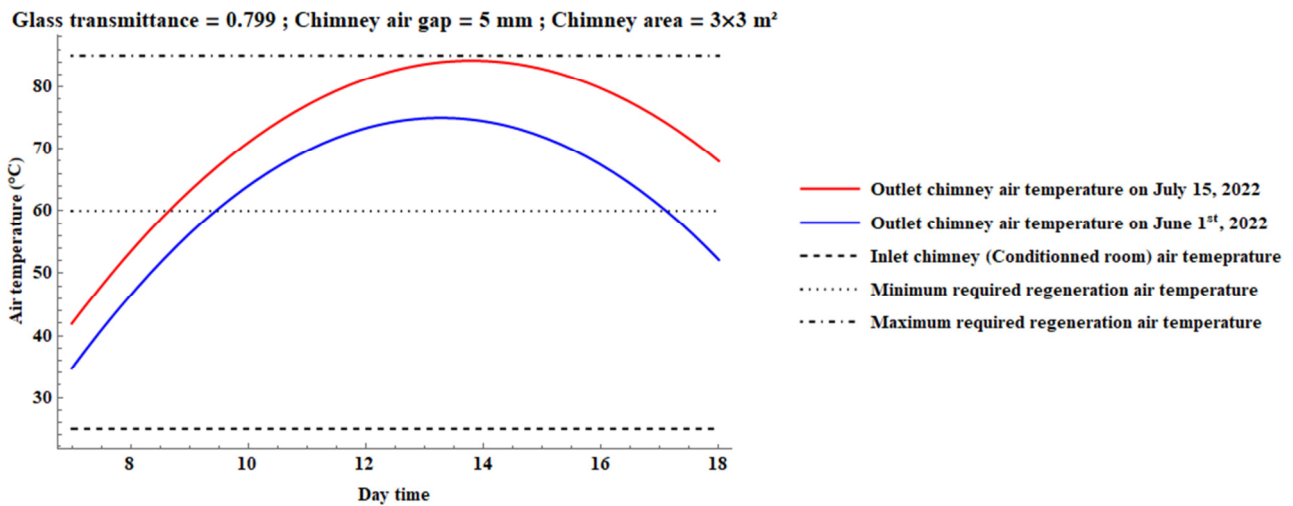

Fig. 4.   Numerical analysis of the outlet chimney air temperature in the solar ventilation system, June 1st and July 15th, 2022.
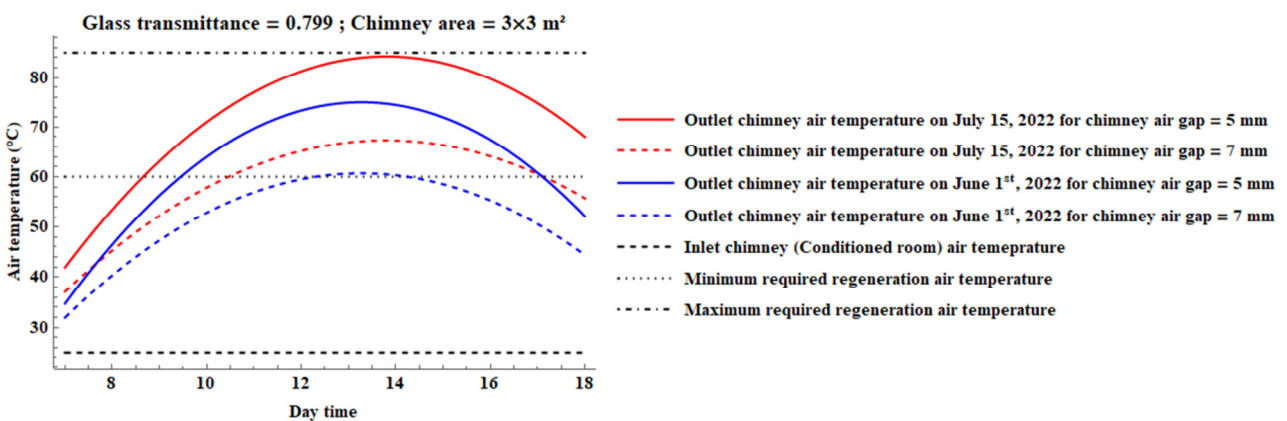

Fig. 5.   Numerical analysis of the impact of the chimney air gap on the outlet chimney air temperature in the solar ventilation system on June 1 and July 15, 2022 in Bisha, Saudi Arabia.
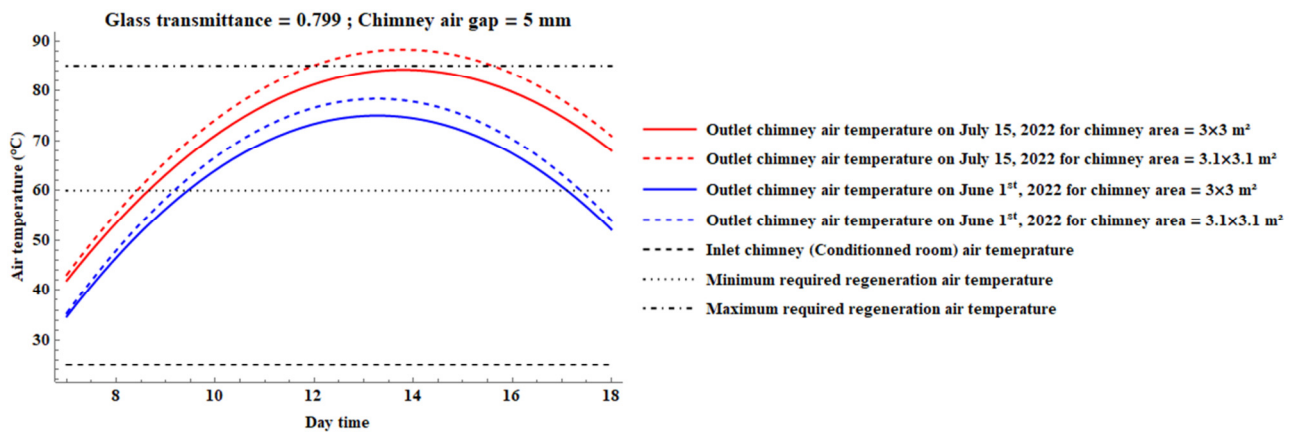
Fig. 6.   Numerical analysis of the impact of the chimney area on the outlet chimney air temperature in the solar ventilation system, on June 1 and July 15, 2022 in Bisha, Saudi Arabia.
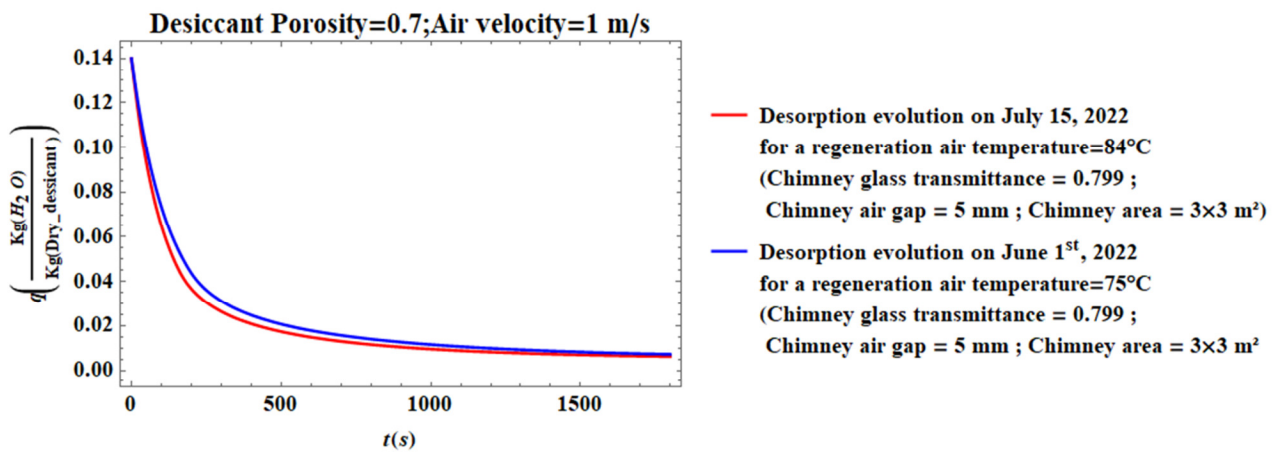

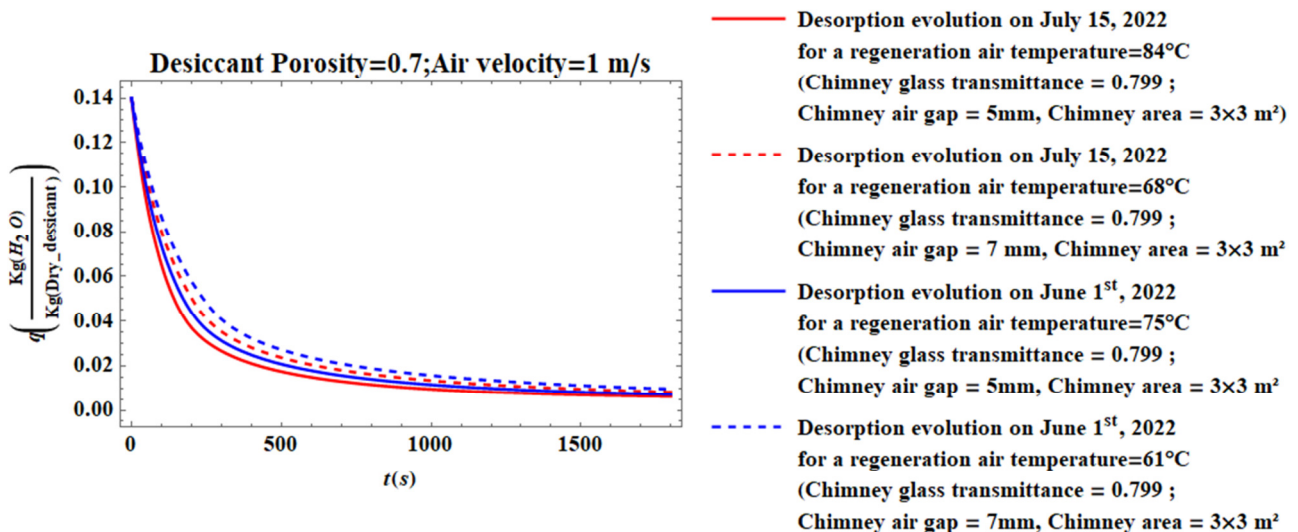Fig. 7.   Desorption evolution in the solar chimney system.

Fig. 8.   The impact of chimney air gap on the desorption rate in the solar chimney system.

Figure 5 provides information regarding the effect of chimney air gap on the thermal performance of the solar chimney in terms of outlet air temperature. The chimney air gap was varied from 5 mm to 7 mm during the two

investigation days: June 1 and July 15, 2022. The glass transmittance and chimney area were set to 0.799 and 3×3 m², respectively. According to Figure 5, on June 1st, 2022, increasing the chimney air gap from 5 mm to 7 mm resulted in a drastic reduction in the outlet chimney air temperature. The maximum air temperature reduction recorded was in the order of 14°C (from 75°C to 61°C), and the outlet chimney air temperature became totally outside the appropriate range of the required regeneration air temperature. This reduction in the outlet chimney air temperature is expected since increasing the chimney air gap reduces the air flow, leading to reduced heating and ventilation effectiveness.

Figure 6 provides information regarding the effect of chimney area on the thermal performance of the solar chimney in terms of outlet air temperature. The chimney area was varied from 3×3 m² to 3.1×3.1 m² for the same study period. The glass transmittance and chimney air gap were set to 0.799 and 5 mm, respectively. According to Figure 6, on June 1st, 2022, increasing the chimney area from 3×3 m² to 3.1×3.1 m² induced a moderate increase in the outlet chimney air temperature, which became more and more within the appropriate range of the required regeneration air temperature. The maximum air temperature increase recorded was in the order of 4°C (from 75°C to 79°C). On July 15th, 2022, increasing the chimney area from 3×3 m² to 3.1×3.1 m² induced a moderate increase in the outlet chimney air temperature but led to a slight exceeding of the outlet chimney air temperature evolution outside the appropriate range of the required regeneration air temperature. The maximum air temperature increase recorded was in the order of 5°C (from 84°C to 89°C). This increase in the outlet chimney air temperature is expected since increasing the chimney area enhances the heat transfer between the absorber and the air.

Overall, the results suggest that a chimney area in the order of 3×3 m² is appropriate to achieve an acceptable thermal performance in terms of hot air regeneration for the desiccant medium within the dehumidification stage. However, a chimney area around 3.1×3.1 m² should be avoided when solar irradiance and ambient temperature are highly intense because it can lead to a slight exceeding of the outlet chimney air temperature outside the appropriate range of the required regeneration air temperature. It is important to note that the appropriate chimney area can vary depending on various factors such as the climate, the solar irradiance, and the size of the conditioned room. Therefore, it is recommended to perform a thorough analysis and simulation under different operating conditions to determine the optimal chimney area for a specific application. Overall, Figure 6 provides important information about the effect of chimney area on the thermal performance of the solar chimney and can be used to optimize the system's operation to maintain a comfortable room temperature while minimizing energy consumption.

Figure 7 principally depicts the evolution of the desiccant moisture content within the dehumidification stage on June 1 and July 15, 2022 from 07:00 to 18:00. The glass transmittance, the chimney air gap and the chimney area are set at 0.799, 5 mm and 3×3 m², respectively. The desiccant desorption rate becomes slightly more pronounced when the

regeneration air temperature increases by 9°, from 75°C to 84°C. The moisture content drops below 0.01 kg (H_2O)/kg (dry desiccant) from 900 s and 1100 s for a regeneration air temperature around 84°C to 75°C respectively. It can be concluded that even if the increase in regeneration air temperature is important, the increase in desiccant desorption rate remains not significant.

Figure 8 provides information regarding the effect of the chimney air gap on the rate of desiccant desorption during the dehumidification stage. The chimney air gap changed from 5 to 7 mm during the two inquiry days. The chimney area and glass transmittance were set as 33 m² and 0.799 m², respectively. According to Figure 8, on June 1st, 2022, the increment of the chimney air gap from 5 mm to 7 mm resulted in a moderate decline in the desiccant desorption rate. For regeneration air temperatures ranging from around 75°C to 61°C, the moisture content decreased to less than 0.01 kg (H_2O)/kg (dry desiccant) in the 1100 s and 1700 s, respectively. On July 15, 2022, increasing the chimney air gap from 5 mm to 7 mm also resulted in a moderate decline in the desiccant desorption rate. From 900 s and 1400 s, with a regeneration air temperature ranging from 84°C to 68°C, respectively, the moisture content fell below 0.01 kg (H2O)/kg (dry desiccant). Overall, the results suggest that increasing the chimney air gap from 5 mm to 7 mm can lead to a moderate decline in the rate of desiccant desorption during the dehumidification stage. However, the reduction in the desiccant desorption rate is still within an acceptable range, and the moisture content falls below the required level for dry desiccant. It is important to note that the appropriate chimney air gap can vary depending on various factors such as the climate, solar irradiance, and the size of the conditioned room. Therefore, it is recommended to perform a thorough analysis and simulation under different operating conditions to determine the optimal chimney air gap for a specific application. Overall, Figure 8 provides important information about the effect of chimney air gap on the rate of desiccant desorption during the dehumidification stage and can be used to optimize the system's operation to maintain a comfortable room temperature while minimizing energy consumption.

IV. CONCLUSIONS

A new solar chimney design with a lateral (vertical) portion is proposed to provide winter mode thermal comfort in a ventilated room. The objective of this study was to conduct a numerical analysis of the thermal and ventilation capabilities of a small-scale hybrid solar ventilation-air conditioning system during two summer days in Bisha, Saudi Arabia. The results of this study will help the optimization of the design of the solar chimney and improving its performance.

To further enhance the sustainability of the suggested design, future technological investigations can be undertaken to examine the coupling between solar ventilation and photovoltaic electricity generation. The integration of these two systems can increase the overall energy efficiency of the building and reduce its carbon footprint. Additionally, experimental studies of the suggested hybrid design, alone or in combination with photovoltaic electricity generation, can be

carried out to validate the results of the numerical analysis and identify any potential areas for improvement.

Overall, the proposed solar chimney design with a lateral (vertical) portion has the potential to provide winter mode thermal comfort in a ventilated room while also reducing energy consumption and carbon emissions. Further research and development in this area can lead to the creation of more sustainable and energy-efficient buildings.

ACKNOWLEDGEMENT

REFERENCES

[1] G. Angrisani, C. Roselli, and M. Sasso, "Effect of rotational speed on the performances of a desiccant wheel," *Applied Energy*, vol. 104, pp. 268–275, Apr. 2013, https://doi.org/10.1016/j.apenergy.2012.10.051.

[2] E. P. Sakonidou, T. D. Karapantsios, A. I. Balouktsis, and D. Chassapis, "Modeling of the optimum tilt of a solar chimney for maximum air flow," *Solar Energy*, vol. 82, no. 1, pp. 80–94, Jan. 2008, https://doi.org/10.1016/j.solener.2007.03.001.

[3] J. Yau, J. J. Wei, H. Wang, O. Eniola, and F. P. Ibitoye, "Modeling of the Internal Temperature for an Energy Saving Chinese Solar Greenhouse," *Engineering, Technology & Applied Science Research*, vol. 10, no. 5, pp. 6276–6281, Oct. 2020, https://doi.org/10.48084/etasr.3728.

[4] S. Alimi, R. Nciri, F. Nasri, Y. A. Rothan, and C. Ali, "Performance investigation of an original hybrid solar façade system used for HDH desalination and building natural ventilation," *Journal of Building Engineering*, vol. 42, Oct. 2021, Art. no. 102515, https://doi.org/10.1016/j.jobe.2021.102515.

[5] F. Nasri, F. Alqurashi, R. Nciri, and C. Ali, "Design and simulation of a novel solar air-conditioning system coupled with solar chimney," *Sustainable Cities and Society*, vol. 40, pp. 667–676, Jul. 2018, https://doi.org/10.1016/j.scs.2018.04.012.

[6] R. Bassiouny and N. S. A. Korah, "Effect of solar chimney inclination angle on space flow pattern and ventilation rate," *Energy and Buildings*, vol. 41, no. 2, pp. 190–196, Feb. 2009, https://doi.org/10.1016/j.enbuild.2008.08.009.

[7] A. Oudrane, B. Aour, B. Zeghmati, X. Chesneau, and H. Massaoud, "Study and Simulation of the Density of the Incident Solar Flux on the Walls of a Building in Adrar, Algeria," *Engineering, Technology & Applied Science Research*, vol. 7, no. 5, pp. 1940–1945, Oct. 2017, https://doi.org/10.48084/etasr.1337.

[8] W. Liping and L. Angui, "A numerical study of vertical solar chimney for enhancing stack ventilation in buildings," in *The 21th Conference on Passive and Low Energy Architecture*, Eindhoven, The Netherlands, Sep. 2004.

[9] C. R. Ruivo, J. J. Costa, A. R. Figueiredo, and A. Kodama, "Effectiveness parameters for the prediction of the global performance of desiccant wheels – An assessment based on experimental data," *Renewable Energy*, vol. 38, no. 1, pp. 181–187, Feb. 2012, https://doi.org/10.1016/j.renene.2011.07.023.

[10] C. R. Ruivo, J. J. Costa, and A. R. Figueiredo, "Numerical study of the influence of the atmospheric pressure on the heat and mass transfer rates of desiccant wheels," *International Journal of Heat and Mass Transfer*, vol. 54, no. 7, pp. 1331–1339, Mar. 2011, https://doi.org/10.1016/j.ijheatmasstransfer.2010.12.008.

[11] A. Fouda, H. Elattar, S. Rubaiee, A. S. B. Mahfouz, and A. M. Alharbi, "Thermodynamic and Performance Assessment of an Innovative Solar-Assisted Tri-Generation System for Water Desalination, Air-Conditioning, and Power Generation," *Engineering, Technology & Applied Science Research*, vol. 12, no. 5, pp. 9316–9328, Oct. 2022, https://doi.org/10.48084/etasr.5237.

[12] A. Y. K. Tan and N. H. Wong, "Influences of ambient air speed and internal heat load on the performance of solar chimney in the tropics,"

[13] *Solar Energy*, vol. 102, pp. 116–125, Apr. 2014, https://doi.org/10.1016/j.solener.2014.01.023.

[13] J. Arce, M. J. Jiménez, J. D. Guzmán, M. R. Heras, G. Alvarez, and J. Xamán, "Experimental study for natural ventilation on a solar chimney," *Renewable Energy*, vol. 34, no. 12, pp. 2928–2934, Dec. 2009, https://doi.org/10.1016/j.renene.2009.04.026.

[14] A. P. Haghighi and M. Maerefat, "Solar ventilation and heating of buildings in sunny winter days using solar chimney," *Sustainable Cities and Society*, vol. 10, pp. 72–79, Feb. 2014, https://doi.org/10.1016/j.scs.2013.05.003.

[15] S. Mehranfar, A. Gharehghani, A. Azizi, A. Mahmoudzadeh Andwari, A. Pesyridis, and H. Jouhara, "Comparative assessment of innovative methods to improve solar chimney power plant efficiency," *Sustainable Energy Technologies and Assessments*, vol. 49, Feb. 2022, Art. no. 101807, https://doi.org/10.1016/j.seta.2021.101807.

[16] Y. Kassem, H. Gokcekus, and F. A. R. Agila, "Techno-Economic Feasibility Assessment for the promotion of Grid-Connected Rooftop PV Systems in Botswana: A Case Study," *Engineering, Technology & Applied Science Research*, vol. 13, no. 2, pp. 10328–10337, Apr. 2023, https://doi.org/10.48084/etasr.5668.

[17] M. Shatat, M. Worall, and S. Riffat, "Opportunities for solar water desalination worldwide: Review," *Sustainable Cities and Society*, vol. 9, pp. 67–80, Dec. 2013, https://doi.org/10.1016/j.scs.2013.03.004.

[18] A. Al-Karaghouli and L. L. Kazmerski, "Energy consumption and water production cost of conventional and renewable-energy-powered desalination processes," *Renewable and Sustainable Energy Reviews*, vol. 24, pp. 343–356, Aug. 2013, https://doi.org/10.1016/j.rser.2012.12.064.

[19] C. Li, Y. Goswami, and E. Stefanakos, "Solar assisted sea water desalination: A review," *Renewable and Sustainable Energy Reviews*, vol. 19, pp. 136–163, Mar. 2013, https://doi.org/10.1016/j.rser.2012.04.059.